

Ab initio study of Z_2 topological phases in perovskite (111) $(\text{SrTiO}_3)_7/(\text{SrIrO}_3)_2$ and $(\text{KTaO}_3)_7/(\text{KPtO}_3)_2$ multilayers

J. L. Lado,^{1,2,*} V. Pardo,^{1,2,†} and D. Baldomir^{1,2}

¹ *Departamento de Física Aplicada, Universidade de Santiago de Compostela, E-15782 Santiago de Compostela, Spain*

² *Instituto de Investigaciones Tecnológicas, Universidade de Santiago de Compostela, E-15782 Santiago de Compostela, Spain*

(Dated: October 31, 2018)

Honeycomb structures formed by the growth of perovskite 5d transition metal oxide heterostructures along the (111) direction in t_{2g}^5 configuration can give rise to topological ground states characterized by a topological index $\nu=1$, as found in Nature Commun. 2, 596 (2011). Using a combination of a tight binding model and ab initio calculations we study the multilayers $(\text{SrTiO}_3)_7/(\text{SrIrO}_3)_2$ and $(\text{KTaO}_3)_7/(\text{KPtO}_3)_2$ as a function of parity asymmetry, on-site interaction and uniaxial strain and determine the nature and evolution of the gap. According to our DFT calculations, $(\text{SrTiO}_3)_7/(\text{SrIrO}_3)_2$ is found to be a topological semimetal whereas $(\text{KTaO}_3)_7/(\text{KPtO}_3)_2$ is found to present a topological insulating phase that can be understood as the high U limit of the previous one, that can be driven to a trivial insulating phase by a perpendicular external electric field.

I. INTRODUCTION

Topological insulators (TI)^{1,2} are a type of materials which show a gapped bulk spectrum but gapless surface states. The topological nature of the surface states protects them against perturbations and backscattering.³⁻⁹ In addition, the surface of a d-dimensional TI is such that the effective Hamiltonian defined on its surface cannot be represented by the Hamiltonian of a d-1 dimensional material with the same symmetries, so the physics of a (d-1)-surface of a topological insulator may show completely different behavior from that of a conventional (d-1)-dimensional material. Surface states¹⁰ can be understood in terms of solitonic states which interpolate between two topologically different vacuums, the topological vacuum of the TI and the trivial vacuum of a conventional insulator or empty space.

The ground state of a system can be classified by a certain topological number^{11,12} depending on its dimensionality and symmetries present which define its topological classification.^{2,13} Two-dimensional single-particle Hamiltonians with time reversal (TR) invariance are classified in a Z_2 ($\nu = 0, 1$) topological class.¹² Two-dimensional TR systems with nontrivial topological index ($\nu = 1$) show the so-called quantum spin Hall effect (QSHE) which is characterized by a non-vanishing spin Chern number¹⁴ and a helical edge current.¹⁵ This state has been theoretically predicted and experimentally con-

firmed in HgTe quantum wells,¹⁶⁻¹⁸ as well as predicted in several materials such as two-dimensional Si and Ge¹⁹ and transition metal oxide (TMO) heterostructures.²⁰ All these systems have in common that they present a honeycomb lattice structure with two atoms (A,B) as atomic basis. In that situation, it is tempting to think that the effective Hamiltonian in certain k-points could have the form of a Dirac Hamiltonian. The components of the spinor would be some combination of localized orbitals in the A or B atoms, whereas the coupling would take place via non-diagonal elements due to the bipartite geometry of the lattice. The simplest and best known example is graphene, where the Hamiltonian is a Dirac equation in two nonequivalent points K and K'. At half filling, graphene with TR and inversion symmetry (IS) has $\nu = 1$,²¹ so a term which does not break those symmetries and opens a gap in the whole Brillouin zone would give rise to the QSHE state. The way in which an IS term can arise in a graphene Hamiltonian is due to spin-orbit coupling (SOC), however it is known that the gap opened this way is too small.²² In contrast, a sublattice asymmetry, which breaks IS, will open a trivial gap, as in BN.^{23,24}

How a honeycomb structure can be constructed from a perovskite unit cell can be seen in Fig. 1a and 1b, a perovskite bilayer grown along the (111) direction made of an open-shell oxide is sandwiched by an isostructural band insulating oxide. The metal atoms of the bilayer form a buckled honeycomb

lattice. It has been shown that perovskite (and also pyrochlore) (111) multilayers can develop topological phases,^{20,25–30} as well as spin-liquid phases and non-trivial superconducting states.³¹ Topological insulating phases have been predicted for various fillings of the d shell,²⁰ here we will focus on the large SOC limit (5d electrons) and formal d^5 filling. We will study two different multilayers, $(\text{SrTiO}_3)_7/(\text{SrIrO}_3)_2$ and $(\text{KTaO}_3)_7/(\text{KPtO}_3)_2$ and we will focus on the realization of a nontrivial $\nu = 1$ ground state. SrIrO_3 ($a_{\text{SrIrO}_3} = 3.94 \text{ \AA}$)³² is a correlated metal³³ whose lattice match with SrTiO_3 (STO) would be close enough ($a_{\text{SrTiO}_3} = 3.905 \text{ \AA}$)³⁴ for them to grow epitaxially with standard growth techniques.³⁵ KPtO_3 has not been synthesized (to the best of our knowledge) but our calculations ($a_{\text{KPtO}_3} = 4.02 \text{ \AA}$) show a reasonable lattice match with KTaO_3 would be possible ($a_{\text{KTaO}_3} = 3.98 \text{ \AA}$).³⁶ The first multilayer is an iridate very similar to the well known Na_2IrO_3 .^{37–39} This system presents a layered honeycomb lattice of Ir atoms at t_{2g}^5 filling, whereas the present bilayers show a buckled honeycomb lattice, and is predicted to develop the QSHE, however electron correlation would lead to an antiferromagnetic order in the edges. We will study the dependence of the topological ground state on the applied uniaxial strain and the electron-electron interaction and we will determine a transition between two topological phases in both materials. The work is organized as follows. In Section II we introduce a simple tight binding (TB) model as in Ref. 20 focusing on the t_{2g}^5 case. In Section III we use density functional theory (DFT) calculations to study the evolution of both multilayers with uniaxial strain and on-site Coulomb repulsion and we determine the ground state of each material. In Section IV we study the stability of the topological phase against TR and IS breaking using both TB and DFT calculations. Finally in Section V we summarize the results obtained.

II. TIGHT BINDING MODEL

The qualitative behavior of this system can be understood using a simple TB model for the 5d electrons in the TM atoms, as shown in Ref. 20. In Section IIA we will give the qualitative behavior of the effective Hamiltonian. In Section IIB we will show numerical calculations of the full model.

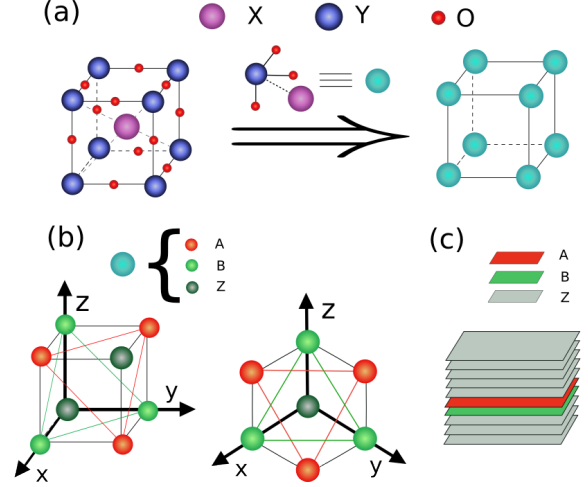


FIG. 1: (Color online) (a) Scheme of the cubic perovskite structure XYO_3 . (b) Construction of the bilayer, the TM atoms are arranged in a triangular A and B lattice in the (111) direction in such a way the two atoms will form a honeycomb lattice. The Z atom corresponds to the insulating layer (in our case SrTiO_3 or KTaO_3) and does not participate in the honeycomb. (c) Scheme of the multilayer considered in the DFT calculations.

A. Full Hamiltonian

The octahedral environment of oxygen atoms surrounding the transition metal atoms decouples the d levels in a t_{2g} sextuplet and an e_g quadruplet. Given that the crystal field gap is higher than the other parameters considered we will retain only the t_{2g} orbitals. The Hamiltonian considered for the t_{2g} levels takes the form

$$H = H_{SO} + H_t + H_{tri} + H_m \quad (1)$$

H_{SO} is the SOC term, which gives rise to an effective angular momentum $J_{eff} = S - L$ which decouples the t_{2g} levels into a filled $j=3/2$ quadruplet and a half filled $j = 1/2$ doublet. H_t is the hopping between neighboring atoms via oxygen that couples the local orbitals. H_{tri} is a local trigonal term²⁰ which is responsible for opening a gap (as we will see below) without breaking TR and IS. H_m is a term which breaks IS making the two sublattices nonequivalent tending to open a trivial gap by decoupling them. In the following discussion we will suppose that this

last term is zero, but we will analyze its role in Section IV.

We are interested in two different regimes as a function of SOC strength: strong and intermediate. We call strong SOC to the regime where the $j=3/2$ and $j=1/2$ are completely decoupled so that there is a trivial gap between them. We will refer to an intermediate regime if the two subsets are coupled by the hopping. The key point to understand the topological character of the calculations is that a t_{2g}^5 configuration can be adiabatically connected from the strong to the intermediate regime without closing the gap. The argument is the following, beginning in the strong SOC regime it is expected that a four-band effective model will be a good approximation. In this regime the mathematical structure of the effective Hamiltonian turns out to be equivalent to graphene. The trigonal term is responsible for opening a gap Δ via a third order process in perturbation theory

$$\Delta \sim \lambda_{tri} \frac{t^2}{\alpha^2} \quad (2)$$

where λ_{tri} is the trigonal coupling, t is the hopping parameter and α the SOC strength. It can be checked by symmetry considerations that the restriction of the matrix representations leads to this term as the first non-vanishing contribution in perturbation theory. Eq. (2) has been checked by a logarithmic fitting of numerical calculations of the full model. This term will open a gap in the K point conserving TR and IS and thus realizing a $\nu = 1$ ground state.²¹

As SOC decreases, the gap becomes larger while the system evolves from the strong to the intermediate regime, so the intermediate regime is expected to be a topological configuration²⁰ with a non-vanishing gap. Note that even though perturbation theory will only hold in the strong SOC regime, the increase in the gap as the system goes to the intermediate regime suggests that the t_{2g}^5 configuration will always remain gapped. This argument is checked by the numerical calculations shown below.

B. Results from tight binding calculations

In Fig. 2 we show the results of a calculation using the TB Hamiltonian proposed above. Figure 2a is

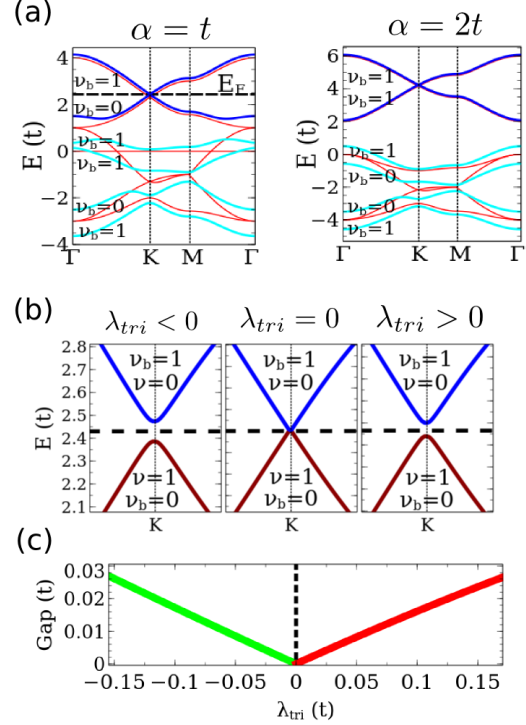


FIG. 2: (Color online) (a) Band structure of the TB model with intermediate $\alpha = t$ (left) and strong $\alpha = 2t$ (right) SOC strength and $\lambda_{tri} = -0.5t$. The difference between the two cases relies on the ν_b invariant of the last filled band. The red lines are the band structure with $\lambda_{tri} = 0$. (b) Band structure zoomed for the $j=1/2$ bands near the K point for negative ($\lambda_{tri} = -0.5t$), zero and positive ($\lambda_{tri} = 0.5t$) trigonal coupling. In the three cases the topological invariant gives a topological ground state. (c) Evolution of the gap in the K point with λ_{tri} for the intermediate SOC regime. The two topological phases found will be identified as HUTI and LUTI in the DFT calculations.

the bulk band structure for strong and intermediate SOC strength α . If a non-vanishing trigonal term is included, it opens a gap in the Dirac points of the band structure generating topologically non-trivial configurations. We can see this clearly in Fig. 2b, where the band structure close to the Fermi level in the vicinity of the K point is shown.

The topological character of each configuration is defined by the ν topological invariant which for a

band in an IS Hamiltonian can be calculated as²¹

$$(-1)^{\nu_b} = \prod_{\text{TRIM}} \langle \Psi_b | P | \Psi_b \rangle \quad (3)$$

where the product runs over the four time reversal invariant momenta (TRIM). The full invariant of a configuration will be the product of the last equation over all the occupied bands

$$\nu = \sum_{\text{occ. bands}} \nu_b \pmod{2} \quad (4)$$

For a t_{2g}^5 filling the first unfilled band has always $\nu_b = 1$ but the difference between strong and intermediate SOC is the ν_b invariant of the last filled band. For strong SOC the $j=1/2$ and $j=3/2$ are completely decoupled so a t_{2g}^4 configuration would be topologically trivial, being the invariant of the fifth band $\nu_b = 1$. However, when SOC is not sizable the bandwidths are large enough to couple the $j=1/2$ and $j=3/2$ levels so that the t_{2g}^4 filling is a topological configuration. In both cases the t_{2g}^5 filling is topologically non-trivial.²⁰ We will see below using DFT calculations that the systems under study (TMO's with 5d electrons in a perovskite bilayer structure) are in this intermediate SOC regime.

Figure 2b shows the bulk band structure, focusing now on the $j=1/2$ bands, for negative, zero and positive trigonal terms. The left numbers are the ν_b invariant of the band while the right numbers are the sum of the invariants of that band and the bands below it. No matter what the sign of λ_{tri} is, the configuration becomes non-trivial, being its role to open a gap in the K point around the Fermi level. In the DFT calculations below, it will be seen that a change of sign of the trigonal term can be understood as a topological transition between a low U topological insulating phase (LUTI) and a high U topological insulator (HUTI), across a boundary where the system behaves as a topological semimetal (TSM).

III. DFT CALCULATIONS

A. Computational procedures

Ab initio electronic structure calculations have been performed using the all-electron full potential code WIEN2K⁴⁰ The unit cell chosen is shown in Fig. 1c. It consists of 9 perovskite layers grown along the

(111) direction, 2 layers of SrIrO₃ (KPtO₃) which conform the honeycomb and 7 layers of SrTiO₃ (KTaO₃) which isolate one honeycomb from the other.

For the different off-plane lattice parameters along the (111) direction of the perovskite considered, the structure was relaxed using the full symmetry of the original cell. The exchange-correlation term is parametrized depending on the case using the generalized gradient approximation (GGA) in the Perdew-Burke-Ernzerhof⁴¹ scheme, local density approximation+U (LDA+U) in the so-called "fully located limit"⁴² and the Tran-Blaha modified Becke-Jonsson (TB-mBJ) potential.⁴³

The calculations were performed with a k-mesh of $7 \times 7 \times 1$, a value of $R_{mt}K_{max} = 7.0$. SOC was introduced in a second variational manner using the scalar relativistic approximation.⁴⁴ The R_{mt} values used were in a.u. 1.89 for Ti, 1.91 for Ir, 2.5 for Sr and 1.67 for O in the (SrTiO₃)₇/(SrIrO₃)₂ multilayer and 1.93 for Ta, 1.92 for Pt, 2.5 for K, 1.7 for O in the (KTaO₃)₇/(KPtO₃)₂ multilayer.

B. Band structure of the non-magnetic ground state

We have already discussed that the systems chosen to study a d^5 filling in a honeycomb lattice with substantial SOC are the multilayers (SrTiO₃)₇/(SrIrO₃)₂ and (KTaO₃)₇/(KPtO₃)₂ formed by perovskites grown along the (111) direction.

First the structure is optimized for different c lattice parameters respecting IS using GGA and without SOC. This means that mainly only the interplanar distances in the multilayers are relaxed. For the energy minimum the band structure is calculated turning on SOC.

The band structure using three exchange-correlation schemes (GGA, LDA+U and TB-mBJ) develops the same structure. The ν_b topological invariant of each band is calculated as in the TB model,²¹ the topological invariant being the sum of the ν invariants over all the occupied bands. Figure 3 shows the band structure calculated with TB-mBJ as well as the ν_b invariants also obtained ab initio. The difference in the curvature of the bands with respect to the result obtained with the TB model is due to the existence of bands near the bottom of

the $j=3/2$ t_{2g} quadruplet which are not considered in the TB Hamiltonian. Each band has double degeneracy due to the combination of TR and IS. At the optimized c , the gap between the last filled and the first unfilled band is located at the corner of the Brillouin zone (K-point). At low c (unstable energetically but attainable via uniaxial compression), GGA predicts that the system can become a metal by closing an indirect gap between the K and M points, however TB-mBJ calculations predict that a direct gap is localized at the K point. For all the calculations the ground state has $\nu = 1$ and thus it develops a topological phase. The last filled band has $\nu_b = 0$ so by comparison with the TB results the system corresponds to the intermediate SOC limit in which the $J_{eff} = 1/2$ and $J_{eff} = 3/2$ are not completely decoupled.³⁹ If a 5d electron system like this is in the intermediate SOC limit, it is hard to imagine how one can build a TMO heterostructure closer to the strong SOC limit (the only simple solution would be to weaken the hopping between the TM somehow to increase the α/t ratio). The first unfilled band has $\nu_b = 1$ as expected since a t_{2g}^6 configuration will be a trivial insulator with a gap opened by the octahedral crystal field.

The way a trigonal field is present in the DFT calculations is mainly in two ways. On one hand, strain along the z direction varies the distance to the first neighbors in that direction, so that the electronic repulsion varies as well. We define this deformation as $\epsilon_{zz} = \frac{c-c_0}{c_0}$ where c_0 is the off-plane lattice constant with lowest energy. On the other hand, an on-site Coulomb repulsion defined on the TM by using the LDA+U method has precisely the symmetry of the bilayer, i.e. trigonal symmetry, so varying in some way the on-site potential (always preserving parity symmetry) will have the effect of a trigonal term in the Hamiltonian (see A.3 for further details).

According to this, it is expected that in a certain regime, variations in ϵ_{zz} can be compensated by tuning U . In this regime, similar to what we discussed above, the system will develop a transition between two topological phases: a LUTI and a HUTI. At even higher U the system will show magnetic order. We will address this point later and by now we will focus first on the non-magnetic (NM) phase. In order to study the phase diagram defined by the parameters ϵ_{zz} and U , we will perform calculations keeping one of them constant and determine how the gap closes as the other parameter varies, keeping track of the

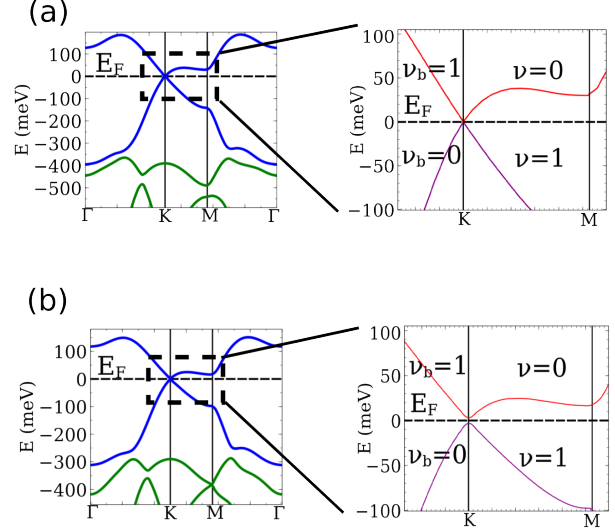


FIG. 3: (Color online) Band structure obtained in the DFT calculations for the optimized lattice parameter c . The calculations were performed with TB-mBJ for both $(\text{SrTiO}_3)_7/(\text{SrIrO}_3)_2$ (a) and $(\text{KTaO}_3)_7/(\text{KPtO}_3)_2$ (b). The right panels are the band structure zoomed in near the Fermi level with the topological invariants displayed. ν_b is the invariant of the band considered calculated by Eq. 3 whereas ν is the sum over all the bands up to the one considered, in Eq. 4.

parities at both sides of the transition.

C. Evolution of the gap with uniaxial strain

Here we will discuss the behavior of the gap in the K point with ϵ_{zz} for various U and J values. First we analyze the behavior of both materials in parameter space showing their similarities finishing characterizing the actual position of the ground state of the system in the general phase diagram.

First we focus on the $(\text{SrTiO}_3)_7/(\text{SrIrO}_3)_2$ case. As shown in Figure 4a, the gap closes as a function of c , so uniaxial strain can drive the system between two insulating phases just as λ_{tri} does in the TB model. However, for high U (see below the discussion on the plausible U values) the transition point disappears (two such cases are plot in Fig. 4a). For low U (see Figs. 4 c,d), ϵ_{zz} can drive the system from a positive trigonal term to a negative one. This means that uniaxial strain can change the sign of the

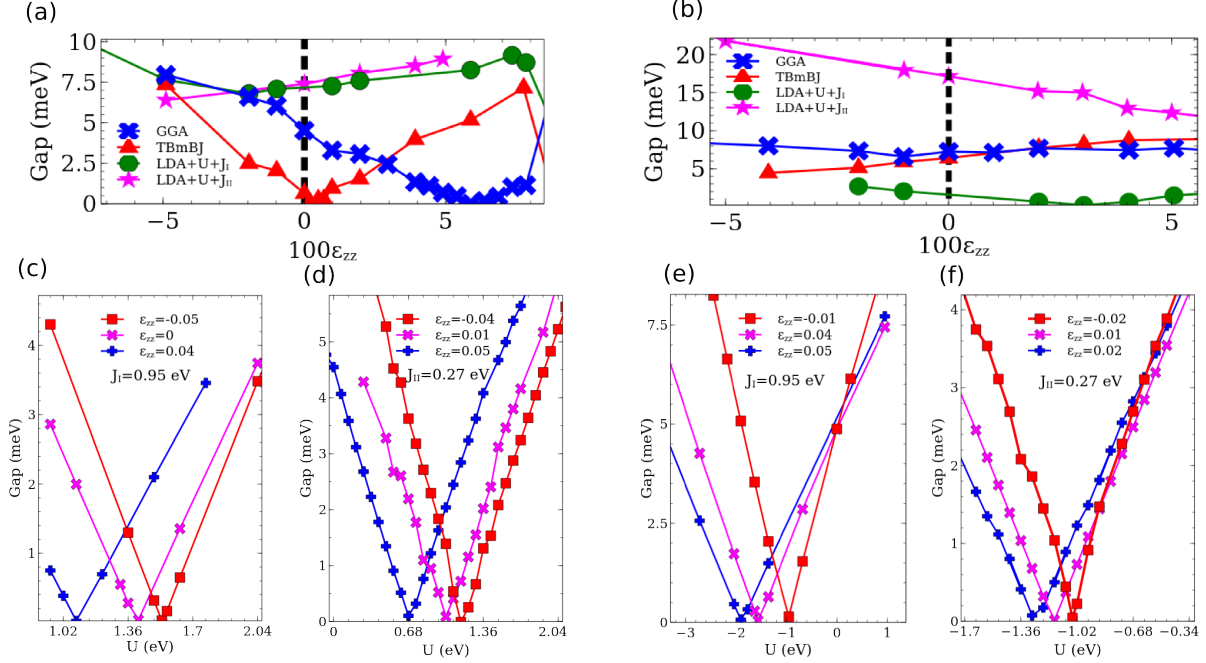


FIG. 4: (Color online) Evolution of the gap as a function of the uniaxial strain for the Ir-based multilayer (a) and Pt-based multilayer (b). Evolution of the gap with the on-site interaction for the Ir-based multilayer (c,d) and Pt-based multilayer (e,f) for small (c,e) and large (d,f) J . It is seen that both systems show a similar behavior although in a different U regime. In (a) the values of U, J are $U = 2.7$ eV $J = 0.95$ eV for the circles and $U = 2.3$ eV $J = 0.27$ eV for the stars, in (b) $U = -1.4$ eV $J = 0.95$ eV for the circles and $U = 2.3$ eV $J = 0.27$ eV for the stars.

effective trigonal term of the Hamiltonian. However, for high U (Fig. 4a), strain is not capable of changing the trigonal field, so the system remains in the same topological phase for every ϵ_{zz} . For the calculations using the TB-mBJ scheme (we will see below to what effective U this situation would correspond), the transition point takes place almost at $\epsilon_{zz} = 0$, so based on this scheme, the Ir-based multilayer would be classified rather as a TSM than as a TI.

Now we will focus on the $(\text{KTaO}_3)_7/(\text{KPtO}_3)_2$ system (see Fig. 4 b,e,f). For the GGA calculations the transition with ϵ_{zz} disappears, being the system always in the HUTI phase. If the system is calculated using LDA+ U with U negative (circles in Fig. 4b), the behavior is similar to the previous system and the transition point across a TSM reappears. For more realistic values of U and J (stars in Fig. 4b) the transition point disappears again. Thus, the present system (Pt-based), though isoelectronic and isostructural, can be understood as the strong- U limit of the previous system (Ir-based). The band

gap is larger, which is a sought-after feature of these TI, but not large enough to make it suitable for room temperature applications. We observe that changing J does not vary the overall picture, just displaces slightly the phase diagram in U -space.

D. Evolution of the gap with U at constant ϵ_{zz}

The Hamiltonian felt by the electrons depends also on the on-site Coulomb interaction between them. If the variation in the term of the Hamiltonian that controls it takes place only in the TM atoms, the symmetry of the varying term will have the same local symmetry as the TM atoms, i.e. trigonal symmetry. Thus, it is expected that a variation in U will have a similar effect as λ_{tri} in the TB model, so the gap can also be tuned by the on-site interaction.

Figure 4 c,d,e,f shows the behavior of the gap for both systems in an LDA+ U scheme with $J=0.27$ (realistic) and 0.95 (large) eV as the parameter U is

varied.

The slow increase of the gap with U suggests that the gap opened is not that of a usual Mott insulator and reminds rather to the slow increase obtained in the TB model. In fact, the calculation of the ν invariant shows again a topological phase on both sides of the transition.

Both systems develop a transition between the LUTI to the HUTI by increasing U . However, the transition point of $(\text{SrTiO}_3)_7/(\text{SrIrO}_3)_2$ is at positive U 's, for the $(\text{KTaO}_3)_7/(\text{KPtO}_3)_2$ the transition appears at negative U 's, so for all possible reasonable U values the system will be in the HUTI phase.

TB-mBJ calculations have proven to give accurate results of band gaps in various systems,^{46–49} including s-p semiconductors, correlated insulators and d systems, however it might give an inaccurate position of semicore d orbitals⁴⁷ and overestimate magnetic moments for ferromagnetic metals.⁴⁸ For $(\text{SrTiO}_3)_7/(\text{SrIrO}_3)_2$ it is possible to use the transition between the LUTI and the HUTI with the TB-mBJ scheme to estimate which value of U should be used in an LDA+ U calculation for these 5d systems to reproduce the result of the TB-mBJ calculation. The actual value of U needed for a correct prediction of the properties under study is often a matter of contention when dealing with insulating oxides containing 5d TM's.^{37,45} From Fig. 4 c,d it can be checked that the gap closes at $U=1.4$ eV for $J=0.95$ eV and at $U=1.0$ eV for the more realistic $J=0.27$ eV, so this suggests that the values which might be used in an LDA+ U calculation to mimic the TB-mBJ result (a zero gap at $\epsilon_{zz} = 0$) are on the order of $U = 1.0$ eV in agreement with Ref. 39. Other works relate to a value of U on the order of 2 eV,^{50,51} however due to the well known property dependence of the value of U ,⁵² it is still unclear which is the correct value to study these topological phases. Therefore, our result can serve as a reference for other ab initio based phase diagrams for iridates where topological phases have been predicted as a function of U .⁴⁵ Moreover, we study this system in a broad range of U values and using different exchange-correlation schemes to provide a broad picture of the system, rather than using a fixed U value that would yield a more restricted view of the problem.

For the Pt-based multilayer we could also consider the hypothetical effective value for which gap would close at negative U ($U_{eff} = U - J$) for both values

of J , we obtain the values $U_{eff} = -1.42$ eV for $J = 0.27$ eV and $U_{eff} = -2.1$ eV for $J = 0.95$. So, it is clearly seen that the gap of these systems is not only dependent on the parameter $U - J$, but also has a strong dependence on J , both in the realistic picture of the Ir-based multilayer as well as in the negative U regime of the Pt-based multilayer.

Recently topological phases dominated by interactions, called topological Mott insulating phases, have been theoretically found,^{53,54} being this term employed for physically different phenomena. In the HUTI phase, the topological gap of the systems is enhanced by increasing the U parameter so that the system seems to be robust against electron-electron interactions. In the same fashion a usual band insulator can be connected to a Mott insulating phase,^{55,56} the previous robustness suggests that the HUTI phase might be adiabatically connected to a Z_2 non-trivial interacting topological phase.^{57,58} Whether this is an artifact of the DFT method or an acceptable mean field approach of a many body problem is something that can only be clarified with experiments.

IV. STABILITY OF THE TOPOLOGICAL PHASE

So far we have considered a system with both TR and IS. However, given that the Z_2 classification is valid only for TR invariant systems it is necessary to determine if the ground state possesses this symmetry. IS breaking could destroy the topological phase opening a trivial gap by decoupling both sublattices, as would happen if the honeycomb is sandwiched by two different materials.²⁰ TR symmetry breaking will be fulfilled by a magnetic ground state whereas IS breaking will be realized by a structural instability. In this Section we will study the two possibilities and conclude that both systems are structurally stable and remain NM according to TB-mBJ in their ground states.

A. Stability of time reversal symmetry

Increasing electronic interactions will drive the NM ground state to a magnetic trivial Mott insulating phase at very high U . For a magnetic d^5 $S=1/2$ localized-electron system, from Goode-

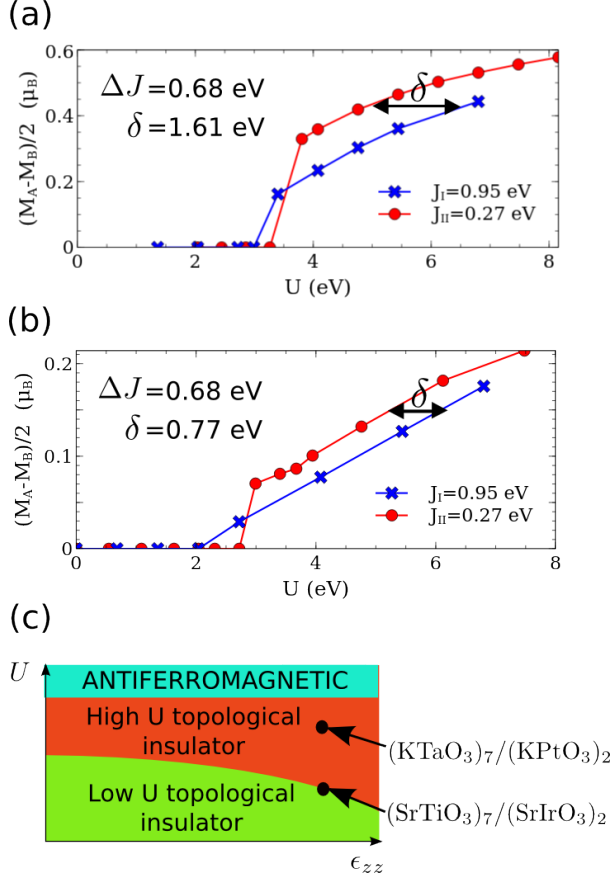


FIG. 5: (Color online) Difference of the sublattice magnetization for the $(\text{SrTiO}_3)_7/(\text{SrIrO}_3)_2$ (a) and $(\text{KTaO}_3)_7/(\text{KPtO}_3)_2$ (b) as a function of U for two different J . (c) Phase diagram in ϵ_{zz} - U space, the approximate position of the ground state of both systems according to TB-mBJ is indicated. At high U the systems develop an AF order, however at realistic U 's both systems remain non-magnetic.

nough's rules⁵⁹ an antiferromagnetic (AF) exchange between the two sublattices is expected which would create an AF ground state breaking both TR and IS. To check this result, we have performed DFT calculations within an LDA+ U scheme taking $J_I = 0.95$ eV and $J_{II} = 0.27$ eV and varying U . For both systems the calculations have been carried out at different U 's for the NM and AF configurations at the two J 's. In both cases the ground state is AF at high U . Also, the sublattice magnetization increases with U . Figures 5a and 5b show the evolution of the

sublattice magnetic moment for both compounds.

Also, a ferromagnetic (FM) phase has been analyzed, being the least preferred one. In the Ir compound a FM phase can be stabilized but has always higher energy than the NM or AF. In the Pt compound a FM phase could not be stabilized for any of the U values considered. The true ground state of the system would be a TI phase in the Pt-based multilayer (or TSM in the Ir-based multilayer according to TBmBJ) depending on the value of U employed, so if the correct value to be used is larger than the critical value (of about 3 eV, which is large according to our previous discussions), the topological Z_2 phase will break down and the Kramers protection of the gapless edge states will disappear; whether the edge states would become gapped or not requires further study. Thus the experimental measurement of the magnetic moment of the ground state of these bilayers would shed light into the correct value of U which should be used in these and other similar compounds. In the Pt-based multilayer the sublattice magnetization is almost only dependent on U_{eff} as can be checked by the shifting of the curves (Fig. 5b), however in the Ir-based multilayer there is a stronger dependence on J (Fig. 5a). Again, simplifying the evolution in terms of the effective $U_{eff} = U - J$ is discouraged for these systems according to our results. The non trivial effect of J ⁶⁰ has been also observed in several compounds such as multi-band materials.^{61,62}

To summarize, we have obtained the magnetization of both compounds as a function of U , showing the system shows a NM ground state for both compounds until a certain U (larger than the value of U that would be equivalent to TB-mBJ calculations) where the system becomes AF (see Fig. 5c).

B. Stability of inversion symmetry

The topological properties of this system rely on both TR and IS. Tight-binding calculations predicted that non-invariant parity terms with energy associated of the order of magnitude of the topological gap could eventually drive the topological phase to a trivial one.

First we will discuss the $(\text{SrTiO}_3)_7/(\text{SrIrO}_3)_2$ system. The simplest IS breaking could be driven by a structural instability. To study the structural stability, we have displaced one of the TM atoms from

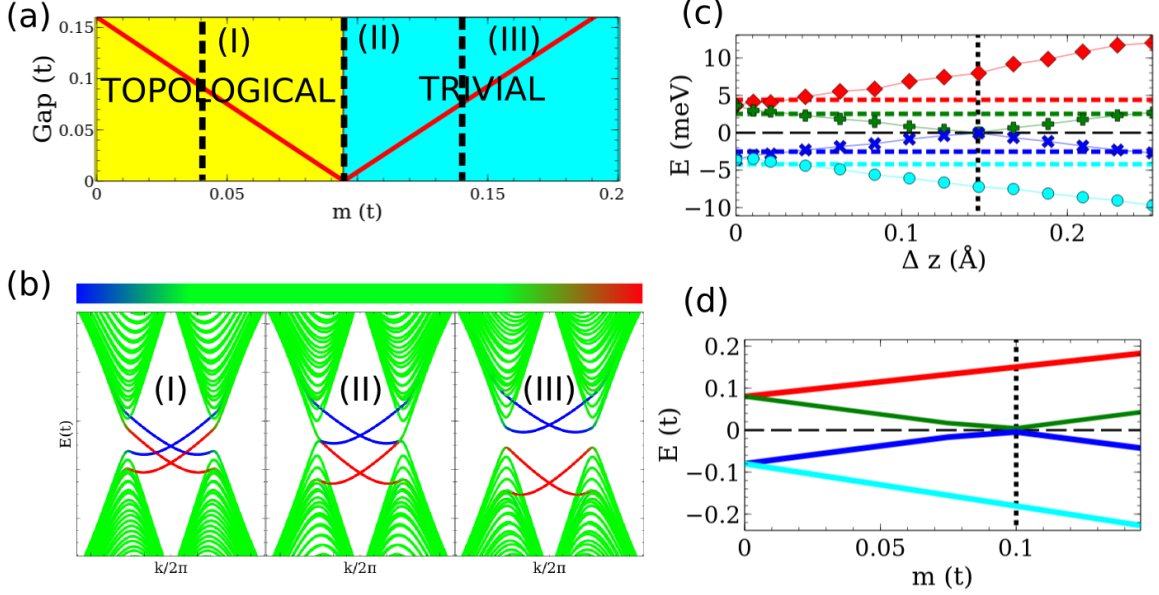


FIG. 6: (Color online) (a) Evolution of the gap in the TB model as a function of m , the closing point marks the transition between topological and trivial phase. (b) Bands of zig-zag ribbons at different m , for low m there are gapless edge states while for large m the edge states become gapped. The color marks the position of the wavefunction, the left edge (blue), the right edge (red) or the bulk (green). (c) Evolution of the eigenvalues obtained in the DFT calculation (using the GGA scheme) of $(\text{KTaO}_3)_7/(\text{KPtO}_3)_2$, the dashed lines correspond to the fully relaxed structure. (d) Evolution of the four eigenvalues closest to the Fermi level for the TB model.

its symmetric position and then relaxed the structure. As a result, the structure returned to the symmetric configuration. However, due to being in the transition point between the two topological phases, any external perturbation (such as a perpendicular electric field) could break inversion symmetry. This system should be classified more as a topological semimetal rather than a topological insulator due to the (almost) vanishing gap of the relaxed structure.

Now we will proceed to $(\text{KTaO}_3)_7/(\text{KPtO}_3)_2$. The first difference between this and the previous system is that in the present case the structure is well immersed in the HUTI phase. A large IS breaking is expected to drive the system to a trivial phase where the sublattices A and B would be decoupled. However, to change its topological class, the system has to cross a critical point where the gap vanishes in some point of the Brillouin zone. According to that, the expected behavior is that the gap closes and reopens as the sublattice asymmetry grows, going from

the original topological phase to a trivial insulating phase.

To check this, we will compare the results obtained from the TB model and DFT calculations. In the TB case, we introduce a new parameter which is a diagonal on-site energy whose value is $+m$ for A atoms and $-m$ for B atoms. This new parameter will break IS and its value will take into account the amount of breaking. When IS is broken the index ν cannot be calculated with the parities at the TRIM's. However, we can study the topological character searching for gapless edge states. For that sake we calculate the band structure of a zig-zag ribbon of 40 dimers width with $\alpha = t$ and $\lambda_{tri} = -t$. The calculations were also carried out in an armchair ribbon and the same behavior is found (not shown), however the mixing of valleys makes the band structure harder to understand. The color of the bands indicates the expectation value of the position along the width of the ribbon of the eigenfunction corresponding to

that eigenvalue, it is checked that the edge states are located in the two edges (red and blue) whereas the rest of the states are bulk states (green). According to the result of the TB model shown in Figs. 6a and 6b, for small m the system remains a topological insulator although the introduction of m weakens the gap. If m keeps increasing the system reaches a critical point where the gap vanishes and if m increases even more the gap reopens but now the edge states become gapped so the system is in a trivial insulating phase.

To model the symmetry breaking in the DFT calculations we move one of the Pt atoms in the z direction. As the distance to the original point increases IS gets more broken. We show the four closest eigenvalues to the Fermi level in the K point for the DFT calculations (Fig. 6c) and TB model (Fig. 6d). For the symmetric structure ($\Delta z = 0$), the combination of TR and IS guarantees that each eigenvalue is two-fold degenerate. Once the atom is moved the degeneracy is broken and the eigenvalues evolve with the IS breaking parameter. The analogy between the two calculations suggests that in the DFT calculation once the gap reopens the new state is also a trivial insulator. The dashed lines in Fig. 6c correspond to the eigenvalues at the K point for the fully relaxed structure allowing IS breaking. Comparing with the curves obtained for the evolution of the eigenvalues it is observed that the relaxed structure is in a slightly asymmetric configuration but it remains in the HUTI phase.

Due to the dependence of the topological state on IS, tuning this behavior would allow to make a device formed by a perovskite heterostructure which can be driven from a topological phase to a trivial phase applying a perpendicular electric field. The device will be formed by the TM honeycomb lattice sandwiched between layers of the same insulating (111) perovskite from above and below. In this configuration the system will be in a HUTI phase. However, a perpendicular electric field will break more the sublattice symmetry inducing a much greater mass term in the Hamiltonian proportional to the applied field. Modifying the value of the electric field it would be possible to drive the system from the topological phase ($\vec{E} = 0$), to the trivial phase (high \vec{E}). This can be exploited as an application of this TI in nanoelectronic and spintronic devices.^{63–66} The sublattice asymmetry needed to make the transition is of the same order of magnitude as the topo-

logical gap, as can be checked in Fig. 6a.

V. SUMMARY

We have studied the gap evolution in the t_{2g}^5 perovskite multilayers $(\text{SrTiO}_3)_7/(\text{SrIrO}_3)_2$ and $(\text{KTaO}_3)_7/(\text{KPtO}_3)_2$ as a function of the on-site Coulomb interactions and uniaxial perpendicular strain conserving time reversal and inversion symmetry. The behavior of the system has been understood with a simple TB model where SOC gave rise to an effective $j=1/2$ four-band Hamiltonian. Uniaxial strain and on-site interactions have been identified as a trigonal term in the TB model whose strength controls the magnitude of a topological gap. The topological invariant ν has been calculated using the parities at the TRIM's both in TB and DFT calculations. Comparisons between the invariants of the bands determines that both of these 5d electron systems stay in the intermediate SOC regime. The small value of the gap in the K-point comes from being a contribution of third order in perturbation theory. In contrast, sublattice asymmetry contributes as a first order term, so the topological phase can be easily destroyed by an external perturbation that gives rise to an IS-breaking term in the Hamiltonian.

$(\text{SrTiO}_3)_7/(\text{SrIrO}_3)_2$ has been found to be a topological semimetal at equilibrium ϵ_{zz} . Comparing TB-mBJ and LDA+U calculations reasonable results can be obtained for U in the range 1 - 2 eV. In $(\text{KTaO}_3)_7/(\text{KPtO}_3)_2$ a HUTI phase at equilibrium has been found. This last system can be driven from topological insulating state to a trivial one by switching on a perpendicular electric field which would break inversion symmetry. Also, we have verified that the properties of these systems are dependent on both U and J instead of only in $U_{eff} = U - J$.

Although the smallness of the gap (less than 10 meV according to TB-mBJ) makes the t_{2g}^5 configuration not particularly attractive for technological applications, the simple understanding of the system turns it physically very interesting. The present system can be thought of as an adiabatic deformation of a mathematical realization of the four band graphene with SOC, with an experimentally accessible gap, the roles of \vec{S} and H_{SO} being played now by \vec{J}_{eff} and H_{tri} , but with a different physical nature of the topological state.

Acknowledgments

The authors thank financial support from the Spanish Government via the project MAT-200908165, and V. P. through the Ramón y Cajal Program. We also thank W. E. Pickett for fruitful discussions.

Appendix A: Tight binding model

In this Section we explain the form of the different terms of the TB Hamiltonian

$$H = H_{SO} + H_t + H_{tri} + H_m \quad (\text{A1})$$

1. Spin-orbit term

We want to obtain the form of the SOC restricted to the t_{2g} subspace. Taking the basis

$$|yz\rangle = \begin{pmatrix} 1 \\ 0 \\ 0 \end{pmatrix} \quad |xz\rangle = \begin{pmatrix} 0 \\ 1 \\ 0 \end{pmatrix} \quad |xy\rangle = \begin{pmatrix} 0 \\ 0 \\ 1 \end{pmatrix} \quad (\text{A2})$$

can be easily seen that the representation $L_i = \hbar l_i$ takes the form

$$l_x = \begin{pmatrix} 0 & 0 & 0 \\ 0 & 0 & i \\ 0 & -i & 0 \end{pmatrix} \quad l_y = \begin{pmatrix} 0 & 0 & i \\ 0 & 0 & 0 \\ -i & 0 & 0 \end{pmatrix} \quad (\text{A3})$$

$$l_z = \begin{pmatrix} 0 & i & 0 \\ -i & 0 & 0 \\ 0 & 0 & 0 \end{pmatrix}$$

The SOC term has the usual form

$$H_{SO} = \frac{2\alpha}{\hbar^2} \vec{L} \cdot \vec{S} = \alpha \vec{l} \cdot \vec{\sigma} \quad (\text{A4})$$

where σ_i are the usual Pauli matrices acting on spin space. The representation follows the commutation relation $[l_i, l_j] = -i\epsilon_{ijk}l_k$ so defining $J_i = S_i - L_i$ the usual commutation relations hold. This change of sign introduces an overall minus sign on the eigenvalues so the spectrum results in a $j = 3/2$ quadruplet with $E_{j=3/2} = -\alpha$ and $j = 1/2$ doublet with $E_{j=1/2} = 2\alpha$.

2. Hopping term

Each site has three bonds directed along the edges of the perovskite structure. The bonds link the A and B sublattices so there will be three different overlaps $t_i = \langle A|H_t|B\rangle$ depending on the direction

$$(t_x, t_y, t_z) = t(\tau_x, \tau_y, \tau_z) \quad (\text{A5})$$

The hopping takes place through the overlap of the t_{2g} orbitals of the TM and the oxygen p orbitals. It can be easily checked that the main contribution gives a matrix form that can be casted in the form

$$(\tau_x, \tau_y, \tau_z) = (l_x^2, l_y^2, l_z^2) \quad (\text{A6})$$

3. Trigonal term

Due to the geometry of the system, a possible term in the Hamiltonian that does not break the spatial symmetries of the system is a trigonal term. This term will differentiate the perpendicular direction from the in-plane directions. This term will behave as an on-site term which mixes the t_{2g} states without breaking the symmetry between them so the general form in the t_{2g} basis is

$$H_{tri} = \lambda_{tri} \begin{pmatrix} 0 & 1 & 1 \\ 1 & 0 & 1 \\ 1 & 1 & 0 \end{pmatrix} \quad (\text{A7})$$

given that the previous matrix is diagonal in the (111) direction, being the perpendicular eigenvalues degenerated, thus preserving the trigonal symmetry.

The way ϵ_{zz} enters in this term is on one hand by anisotropy of charge density due to the lack of local spatial inversion and on the other hand by distortion of the cubic perovskite edges (and thus of the octahedral environment) by expansion/contraction of the (111) direction. The absence of local octahedral rotational symmetry is also responsible for the dependence of λ_{tri} on U. Since varying the onsite interaction will modify the local electron density, provided the local trigonal symmetry is conserved but not the local inversion (as it is broken explicitly by the multilayer), this modification in the electronic density will influence the electrons across the Hartree and exchange-correlation terms, by a term

with those symmetries. In summary, local symmetry forces that a spin-independent perturbation, that includes ϵ_{zz} and spin-independent U-terms, can be recasted on the previous form.

Whether spin-mixing trigonal terms are relevant for the effective model of this system or not should be clarified in the future. Either way, the agreement of the predictions both of the TB model and the DFT calculations, in addition with the explicitly checked topological phase at high U suggests that this model is a well behaved effective model to study the NM phase of this type of systems.

4. Mass term

A term which makes the two sublattices nonequivalent will break inversion symmetry. The minimal term which fulfills this is

$$H_m = ms_z = m \begin{pmatrix} I_A & 0 \\ 0 & -I_B \end{pmatrix} \quad (\text{A8})$$

where I_A and I_B are the identity matrix over the A and B sublattices

-
- * Electronic address: jose.luis.lado@gmail.com
† Electronic address: victor.pardo@usc.es
- ¹ J. E. Moore, *Nature* **464** 194–198 (2010).
 - ² M. Z. Hasan and C. L. Kane, *Rev. Mod. Phys.* **82**, 3045 (2010).
 - ³ L. Fu, C. L. Kane, and E. J. Mele, *Phys. Rev. Lett.* **98**, 106803 (2007).
 - ⁴ D. Hsieh, Y. Xia, L. Wray, D. Qian, A. Pal, J. H. Dil, J. Osterwalder, F. Meier, G. Bihlmayer, C. L. Kane, et al., *Science* **323**, 919 (2009).
 - ⁵ Y. L. Chen, J. G. Analytis, J.-H. Chu, Z. K. Liu, S.-K. Mo, X. L. Qi, H. J. Zhang, D. H. Lu, X. Dai, Z. Fang, et al., *Science* **325**, 178 (2009).
 - ⁶ Y.-Y. Li, G. Wang, X.-G. Zhu, M.-H. Liu, C. Ye, X. Chen, Y.-Y. Wang, K. He, L.-L. Wang, X.-C. Ma, et al., *Advanced Materials* **22**, 4002 (2010).
 - ⁷ H.-M. Guo and M. Franz, *Phys. Rev. B* **81**, 041102 (2010).
 - ⁸ R. R. Biswas and A. V. Balatsky, *Phys. Rev. B* **83**, 075439 (2011).
 - ⁹ X. Zhou, C. Fang, W.-F. Tsai, and J. Hu, *Phys. Rev. B* **80**, 245317 (2009).
 - ¹⁰ A. M. Essin and V. Gurarie, *Phys. Rev. B* **84**, 125132 (2011).
 - ¹¹ D. J. Thouless, M. Kohmoto, M. P. Nightingale, and M. den Nijs, *Phys. Rev. Lett.* **49**, 405 (1982).
 - ¹² C. L. Kane and E. J. Mele, *Phys. Rev. Lett.* **95**, 146802 (2005).
 - ¹³ A. Altland and M. R. Zirnbauer, *Phys. Rev. B* **55**, 1142 (1997).
 - ¹⁴ D. N. Sheng, Z. Y. Weng, L. Sheng, and F. D. M. Haldane, *Phys. Rev. Lett.* **97**, 036808 (2006).
 - ¹⁵ E. Prodan, *Journal of Physics A: Mathematical and Theoretical* **42**, 082001 (2009).
 - ¹⁶ B. A. Bernevig, T. L. Hughes, and S.-C. Zhang, *Science* **314**, 1757 (2006).
 - ¹⁷ M. Knig, S. Wiedmann, C. Brne, A. Roth, H. Buhmann, L. W. Molenkamp, X.-L. Qi, and S.-C. Zhang, *Science* **318**, 766 (2007).
 - ¹⁸ Katja C. Nowack, Eric M. Spanton, Matthias Baenninger, Markus Knig, John R. Kirtley, Beena Kalisky, C. Ames, Philipp Leubner, Christoph Brne, Hartmut Buhmann, Laurens W. Molenkamp, David Goldhaber-Gordon, Kathryn A. Moler, *Nature Materials* **12**, 787 (2013).
 - ¹⁹ C.-C. Liu, W. Feng, and Y. Yao, *Phys. Rev. Lett.* **107**, 076802 (2011).
 - ²⁰ D. Xiao, W. Zhu, Y. Ran, N. Nagaosa, and S. Okamoto, *Nature Communications* **2**, 596 (2011).
 - ²¹ L. Fu and C. L. Kane, *Phys. Rev. B* **76**, 045302 (2007).
 - ²² Y. Yao, F. Ye, X.-L. Qi, S.-C. Zhang, and Z. Fang, *Phys. Rev. B* **75**, 041401 (2007).
 - ²³ M. Topsakal, E. Aktürk, and S. Ciraci, *Phys. Rev. B* **79**, 115442 (2009).
 - ²⁴ G. Giovannetti, P. A. Khomyakov, G. Brocks, P. J. Kelly, and J. van den Brink, *Phys. Rev. B* **76**, 073103 (2007).
 - ²⁵ A. Rüegg and G. A. Fiete, *Phys. Rev. B* **84**, 201103 (2011).
 - ²⁶ K.-Y. Yang, W. Zhu, D. Xiao, S. Okamoto, Z. Wang, and Y. Ran, *Phys. Rev. B* **84**, 201104 (2011).
 - ²⁷ F. Wang and Y. Ran, *Phys. Rev. B* **84**, 241103 (2011).
 - ²⁸ A. Rüegg, C. Mitra, A. A. Demkov, and G. A. Fiete, *Phys. Rev. B* **85**, 245131 (2012).
 - ²⁹ Xiang Hu, Andreas Reg, and Gregory A. Fiee, *Phys. Rev. B* **86**, 235141 (2012).
 - ³⁰ Gang Chen and Michael Hermele, *Phys. Rev. B* **86**, 235129 (2012).
 - ³¹ S. Okamoto, *Phys. Rev. Lett.* **110**, 066403 (2013).
 - ³² F.-X. Wu, J. Zhou, L. Y. Zhang, Y. B. Chen, S.-T. Zhang, Z.-B. Gu, S.-H. Yao, and Y.-F. Chen, *Journal of Physics: Condensed Matter* **25**, 125604 (2013).

- ³³ S. J. Moon, H. Jin, K. W. Kim, W. S. Choi, Y. S. Lee, J. Yu, G. Cao, A. Sumi, H. Funakubo, C. Bernhard, et al., Phys. Rev. Lett. **101**, 226402 (2008).
- ³⁴ M. Schmidbauer, A. Kwasniewski, and J. Schwarzkopf, Acta Crystallographica Section B **68**, 8 (2012).
- ³⁵ I. Hallsteinsen, J. E. Boschker, M. Nord2, S. Lee, M. Rzchowski, P. E. Vullum, J. K. Grepstad, R. Holmestad, C. B. Eom, and T. Tybell J. Appl. Phys. **113**, 183512 (2013).
- ³⁶ J. Narkilahti and M. Tyunina, Journal of Physics: Condensed Matter **24**, 325901 (2012).
- ³⁷ A. Shitade, H. Katsura, J. Kuneš, X.-L. Qi, S.-C. Zhang, and N. Nagaosa, Phys. Rev. Lett. **102**, 256403 (2009).
- ³⁸ R. Comin, G. Levy, B. Ludbrook, Z.-H. Zhu, C. N. Veenstra, J. A. Rosen, Y. Singh, P. Gegenwart, D. Stricker, J. N. Hancock, et al., Phys. Rev. Lett. **109**, 266406 (2012).
- ³⁹ C. H. Sohn, H.-S. Kim, T. F. Qi, D. W. Jeong, H. J. Park, H. K. Yoo, H. H. Kim, J.-Y. Kim, T. D. Kang, Deok-Yong Cho, G. Cao, J. Yu, S. J. Moon, and T. W. Noh Phys. Rev. B **88**, 085125 (2013).
- ⁴⁰ K. Schwarz and P. Blaha, Comp. Mat. Sci. **28**, 259 (2003).
- ⁴¹ J. P. Perdew, K. Burke, and M. Ernzerhof, Phys. Rev. Lett. **77**, 3865 (1996).
- ⁴² V. I. Anisimov, J. Zaanen, and O. K. Andersen, Phys. Rev. B **44**, 943 (1991).
- ⁴³ F. Tran and P. Blaha, Phys. Rev. Lett. **102**, 226401 (2009).
- ⁴⁴ D. J. Singh, *Planewaves, pseudopotentials and LAPW method* (Kluwer Academic Publishers, 1994).
- ⁴⁵ X. Wan, A. M. Turner, A. Vishwanath, and S. Y. Savrasov, Phys. Rev. B **83**, 205101 (2011).
- ⁴⁶ D. J. Singh, Phys. Rev. B **82**, 205102 (2010).
- ⁴⁷ H. Jiang, J. Chem. Phys. **138**, 134115 (2013).
- ⁴⁸ David Koller, Fabien Tran, and Peter Blaha, Phys. Rev. B **83**, 195134 (2011).
- ⁴⁹ A. S. Botana, F. Tran, V. Pardo, D. Baldomir, and P. Blaha, Phys. Rev. B **85**, 235118 (2012).
- ⁵⁰ Cyril Martins, Markus Aichhorn, Log Vaugi, and Silke Bierman, Phys. Rev. Lett. **107**, 266404 (2011).
- ⁵¹ R. Arita, J. Kune, A. V. Kozhevniko, A. G. Eguilu, and M. Imad, Phys. Rev. Lett. **108**, 086403 (2012).
- ⁵² Christoph Loschen, Javier Carrasco, Konstantin M. Neyman, and Francesc Illas Phys. Rev. B **75**, 035115 (2007).
- ⁵³ S. Raghu, X.-L. Qi, C. Honerkamp, and S.-C. Zhang, Phys. Rev. Lett. **100**, 156401 (2008).
- ⁵⁴ L. B. Dmytro Pesin, Nature Physics **6**, 376 (2010).
- ⁵⁵ Andreas Fuhrmann, David Heilmann, and Hartmut Monien, Phys. Rev. B **73**, 245118 (2006).
- ⁵⁶ S. S. Kancharla and S. Okamoto, Phys. Rev. B **75**, 193103 (2007).
- ⁵⁷ Thomas C. Lang, Andrew M. Essin, Victor Gurarie, and Stefan Wessel, Phys. Rev. B **87**, 205101 (2013).
- ⁵⁸ Hsiang-Hsuan Hung, Lei Wang, Zheng-Cheng Gu, and Gregory A. Fiete, Phys. Rev. B **87**, 121113(R) (2013).
- ⁵⁹ J. B. Goodenough, *Magnetism and the chemical bond* (IEEE Press, New York, 2001).
- ⁶⁰ Burak Himmetoglu, Andrea Floris, Stefano de Gironcoli, Matteo Cococcioni, arXiv:1309.3355.
- ⁶¹ L. de Medici, Phys. Rev. B, **83**:205112, (2011).
- ⁶² L. de Medici, J. Mravlje, and A. Georges. Janus-Faced, Phys. Rev. Lett., **107**:256401, (2011).
- ⁶³ P. Michetti and B. Trauzette, Applied Physics Letters **102**, 063503 (2013).
- ⁶⁴ Parijat Sengupta, Tillmann Kubis, Yaohua Tan, Michael Povolotskyi, and Gerhard Klimeck, J. Appl. Phys. **114**, 043702 (2013).
- ⁶⁵ Romeo, F., Citro, R., Ferraro, D., Sassetti, and M., Phys. Rev. B **86**, 165418 (2012).
- ⁶⁶ H. Zhu, C. A. Richter, E. Zhao, J. E. Bonevich, W. A. Kimes, H.-J. Jang, H. Yuan, H. Li, A. Arab, O. Kirillov, et al., Scientific Reports **3** (2013).